RSC Advances

ROYAL SOCIETY OF CHEMISTRY

www.rsc.org/advances

Table of Contents to RSC Advances

Reagent-free Photochemical Silver Dendrite Synthesis on Gallium Nitride Thin Film as a SERS-active Substrate and Catalytic Cluster

Bei Nie[a,b*], Qiuhong Zhou[a] and Weiling Fu[b]

[a.] Chongqing Institute of Green and Intelligent Technology, Chinese Academy of Science, P. R. China

[b.] Department of Clinical Diagnostics and Therapeutics, Xinan Hospital, Third Military Medical University, Chongqing, P. R. China

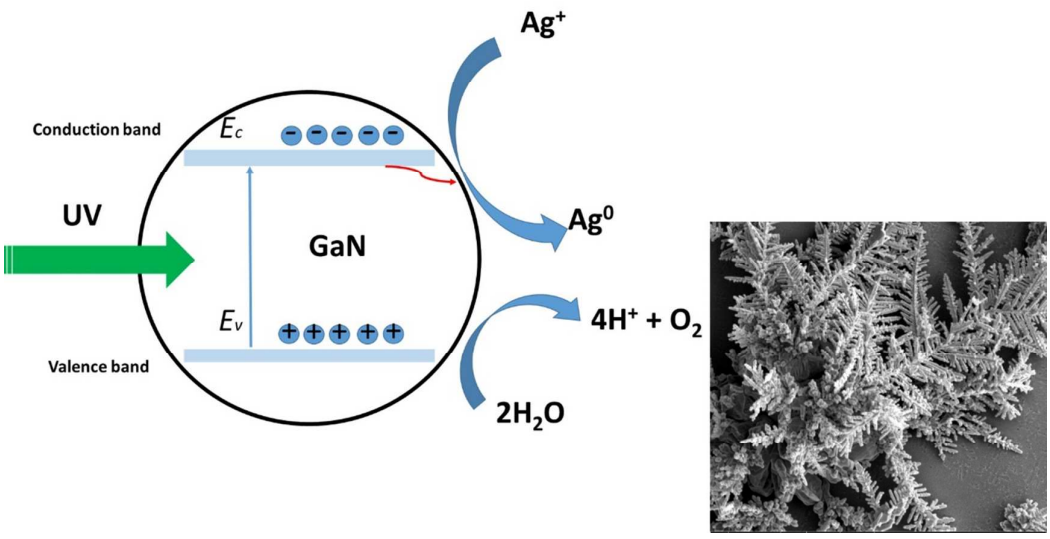

Photochemical approach for dendrite synthesis on GaN Substrate

Reagent-free Photochemical Silver Dendrite Synthesis on Gallium Nitride Thin Film as a SERS-active Substrate and Catalytic Cluster

Bei Nie[a,b*], Qiuhong Zhou[a] and Weiling Fu[b]

[a.] Chongqing Institute of Green and Intelligent Technology, Chinese Academy of Science, P. R. China

[b.] Department of Clinical Diagnostics and Therapeutics, Xinan Hospital, Third Military Medical University, Chongqing, P. R. China

[*]Author to whom correspondence should be addressed, bnie@cigit.ac.cn

Gallium Nitride (GaN) is a compelling semiconductor with a wide bandgap, ~3.4ev, which is essentially important in the development of the blue/green light emitting devices,[1, 2] high power electronics,[3] micro-electro-mechanical systems, high-speed transistors[4] and solar cells.[5] Moreover, the high quality epitaxial GaN film, followed by simple chemical etching produced an exquisite nanoporous architecture, which was extensively applied in optoelectronics, chemical/biochemical sensors and matrix for desorption/ionization mass spectrometry.[6-8] The new research direction recently has been exploited for the supplemental functionality of GaN in photochemical water splitting,[9] pollutant degradation and next-generation electronic/photonic GaN devices,[10] because of its excellent thermal, chemical and optical properties. Relative to its counterparts, GaN, served as a supporting scaffold for catalysts, possesses the intrinsic chemical inertness against extreme harsh reaction conditions, particularly in strong basic and acidic solution.[11]

One of the potential application of GaN is a photoanode for the reduction reaction of metal ion by rendering reductive surface electrons, from which a variety of delicate nanostructures are directly generated on substrate, without the presence of any chemical reagent or surfactant. It thereby provides an alternative green approach for nanoparticle synthesis, friendly to environment and human health.[12] In theory, a wide straddling band provides reductive potential alignment to most redox pairs, including hydrogen generation directly from water. Particularly under continuous uv-irradiation, photoelectrons constantly moved to the conduction band and facilitated the chemical process, giving rise to diverse nanostructures in a

relatively clean and large-scale manner.[13, 14] This hybrid composite possesses many advanced attributes with regard to light scattering, absorption and emission in ways that are not available to either material applied in isolation. For example, a Pt-GaN Schottly diode provides an ultra-sensitive response for hydrogen sensing, on which an order of magnitude improved sensitivity was observed.[15] Ag nanoparticle decorated GaN can significantly amplify spontaneous emission rates on GaN-based LEDs.[16,17,18] Moreover, InGaN/GaN quantum well enhances electron transfer rate, improving photo-current harvest efficiency in GaN solar cells.[19] GaN coated with fine metal nanostructure enables to precisely tune light absorption and scattering. This makes this hybrid system an ideal SERS substrate, as well as a catalytic active sites due to highly reactive surfaces. In addition, the intrinsic chemical inertness and mechanical strength provide the high quality supports for the catalysts, even under harsh conditions, where other alternatives become questionable. Though many methods have been developed for synthesizing branched metal nanostructures using a seed-mediated reaction[20] (CTAB, ascorbic acid,[21] polyvinylpyrrolidone,[22] tris-base(TB),[23] dopamine[24]), they are in a way limited by the principles of fluidic dynamics. It is often a challenge to accurately position products inside the minute apertures, such as nanopores. Direct on-chip synthesis certainly renders an additional dimension to well-disperse active sites throughout supporting surfaces, especially, within tiny compartments. In addition, reductive reagents cause unexpected contaminations on the resulting nanostructures, adversely impacted on the performance of SERS detection and catalytic reaction. Previously, electroless deposition was employed to fabricate nanoparticles in

the interior wall of micropores. However, this approach often involved reductive agents and loaded surfactants to moisturize solid surfaces, which was costly and harmful to the environment.

In this study, we are pursuing to develop a reliable SERS-active GaN substrate using a reagent-free photochemical approach that involves minimal synthesis procedure and few devices. Photon-generated electrons facilitate metal reduction on solid/liquid interface, gradually ossifying to a dendroid nanostructure, the composition of which was experimentally confirmed by the surface based MS analysis (*c.f.* Figure S3†). Our method starts with a n-type GaN thin film deposited on sapphire wafer, approximately 8 μm in thickness with a carrier concentration of 4×10^{18} cm^{-3}. Each wafer was cut into 10 mm × 10 mm square pieces and degreased consecutively in a bath of acetone, ethanol and water. The native oxidation products were removed by 1M hydrofluoric acid in a small plastic container, followed by copious rinsing with DI-water. A drop of aqueous solution of 10 mM $AgNO_3$ (or 10 mM $AuCl_4^-$, in a separated case) was cast on a planar GaN substrate. A 20W low-pressure mercury lamp (Oriel Instruments Model 6182, Oriel Instruments 68806 power supply) was employed as a uv-source for irradiation right above the GaN slide for 3~10 min to produce rugged metal nanostructures.

The dendritic growth mechanism is proposed and briefly depicted by Scheme 1. First, free electrons on GaN surface react with aqueous silver ions, consolidating them into the undiscernible nucleation. This is because the reduction potential of Ag^+/Ag pair (0.799 V vs. standard hydrogen electrode, SHE) is below the GaN valance band. On solid/liquid interface,

conduction and valance bands in GaN (bandgap ~3.4 eV) split to -0.875 eV and 2.525 eV vs. SHE respectively. As formation of surface electric field, density of free electrons, n_s is governed by the following equation (1):

$$n_s = n_0 exp(\frac{-e\Delta\phi_{se}}{k_B T}) \quad (1)$$

where, n_0= 4 × 10^{18} cm^{-3} for n-type GaN crystal and ϕ_{se} represents surface potential derived from band bending. Hence, surface electrons become very reductive, the potential of which is much lower than Ag^+/Ag pair, which induced the galvanic replacement. This facilitates the nucleation process on the solid/liquid interface. Having depleted the surface electrons, further growth Ag structure relies on continuous pumping of electrons out of the conduction band. Noted by Gerischer model[25], uv- photon (wavelength < 360 nm) is totally absorbed by GaN lattice and generates an electron-hole pair, elevating Fermi level and pouring electrons into the solid/liquid interfaces for dendroid growth.

Figure 1 shows the resulting Ag (and Au) dendroid structure profiled by SEM, where a hyper-branched "needle" crystals are observed in a variety of forms, ranging from a "tree-like" spike to a nanoflower. In Ag deposition, typically, dendrites grow slowly and gradually, complying with the model of diffusion-limited aggregation (DLA).[26] Under uv-irradiation, sufficient electrons with high reactivity are driven to conduction bands and migrate to the interface. Hence, the growth rate virtually relies on a random walk of aqueous ion, driven by Brownian motion when it approaches to solid Ag nuclei. It first developed to polyhedral or "rock-like" Ag

nanocubes, in accordance with Volmer-Weber model,[27] producing a large amount of well-dispersed 3D islands throughout the substrate, outlined in Figure 1a. The surface number density of Ag NP is approximately 5×10^7 cm^{-2}. By high magnification SEM image, *i. e.* Figure 2b, the singlet cube is observed with short branched nanowire on jagged rectangles, might because the sharp edge region is more reactive, relative to plain substrate. The wire gradually bifurcated and branched to a dendroid structure with the aid of sufficient surface electrons. A series of SEM micrographs in Figure 2, briefly illustrated this chemical process and morphologic development. The synthesized wires were considered to be many nanometric electrodes, on which electron transfer was favored compared to a planar GaN surface. It thereby produces the oriented crystal growth along the tip and forms a hyper-branched fern structure. Virtually, the rate of crystal growth is determined by molecule diffusion based on random-walking mechanism. The backbone of dendrite attains approximately 3 to 5 μm in length with multiple branches consisting of ~200 nm-in-length projections. These interpenetrated crystals render considerable roughness, vast surface area and most importantly, the vast nanogaps, which provide additional portion for optical enhancement. Finally, the composite of resulting dendrite was verified by surface-based mass analysis, since GaN and Ag grains both can serve as the excellent matrix for laser-induced ionization mass spectrometry.[6] Figure S1† shows the result from surface MS analysis, where Ag element is identified and verified by the presence of Ag^+ cluster ions with unique isotopic patterns (singlet *m/z* 107/109, doublet *m/z* 214/216/218, triplet *m/z* 321/323/325/327) and combined $Ag_nGa_m^+$ adducts). On the other hand, gold

nanoparticles formed a coral-like nanoflower, in accordance with the results from solution-based synthesis.[28] Rather than formation of tree fern, dendroid gold seemingly assembled to a hair-ball structure, illustrated in Figure 1c (low magnification) and Figure 1d (zoom-in image) with approximately 50 to 250 nm crystal tips. The possible development of Au NP is likely following the Volmer-Weber mechanism, in which the crystal growth is mediated by the delicate equilibrium buildup of gold nanoparticles. The continuous growth relies on $AuCl^-$ ion migration and diffusion, which generates dendritic nanocrystals, randomly positioned around a spherical core. Numerous crystal tips radiate from the center and form a flower-like structure, giving rise to disorderly nanoscale roughness and immense surface area. The former, is responsible for Raman enhancement, while the latter counts for widespread catalytic sites over many chemical reactions. To corroborate SERS activity, the heterogeneous GaN chip was incubated in a 100 μM ethanolic 4-aminothiophenol solution, which forms a self-assemble layer through strong Ag-S interaction. In addition, a drop of 1 pmol Rhodamine 6G was directly deposited on the hybrid system prepared for SERS detection. Each optical spectrum was acquired in the range of 500-1400 cm^{-1} with a 10s integration time. Presumably, SERS-active sites are considered to be the interpenetrated branches, especially the apex of crystal tip and overlapped nano-needles.

Figure 3 shows the quality Raman spectra with substantial intensity and great band resolution. In resulting spectrum from 4-ATP and Rhodamine 6G, vibration band caused by aromatic ring and associated substituents are facile being discerned. Peak near 585cm^{-1} dedicates to natural

GaN, Briefly, the dominant peak near 1587 cm^{-1} represents the a_1 ring breathing mode. Two other bands at 1439 and 1394 cm^{-1} are b_2 vibrational modes that result from the Ag-S interaction and which have been implicated in the charge transfer (CT) mechanism for optical enhancement. Peak near 585 cm^{-1} dedicates to natural GaN. In another study, characteristic R6G bands at 612 cm^{-1}, 774 cm^{-1}, 1182 cm^{-1} and 1364 cm^{-1} appear and are easily distinguished from background. The intensities of the two Raman peaks at 612 and 774 cm^{-1}, were assigned to the C-C ring in-plane vibration and the C-H out of plane bending mode. The presence of surface-bounded analyte was further confirmed experimentally by LDI-MS analysis, as illustrated in Figure S1(b)†. The mass-deficit molecular ion, $[ATP-H]^+$ (*m/z* 124.1) was detected directly on hybrid substrate without additional aid of matrix, because GaN and Ag nanoparticle itself both serves as alternative matrix for low weight molecules (<1000Da). The underlying mechanism of special gaseous ion formation was explained by our previous study.[29]

Silver dendrite doubles roles as the catalytic active site and an optical enhancer, which is further demonstrated by a simple chemical approach, in which the starting material and product exhibited a substantial distinction with regard to chemical affinity on metal surfaces. SERS detection reflects and intensifies this discrepancy, because immense optical enhancement often originates from the first-layer analyte on plasmonic network. The analyte that was refractory to coinage metal surfaces produced the negligible signal enhancement, which renders the opportunity of monitoring dynamic catalytic reaction using *in-situ* SERS measurement. A drop of aqueous solution containing 100 µm 4-NP and 5mM BH_4^- was casted

on GaN chip and was covered with glass slide to prevent liquid from evaporation during the reaction. Figure 4 shows the series of resulting Raman spectra, reflecting the progress of catalytic reaction. Initially, 4-NP exhibits a deep yellow color and remains unaltered for quite long time without the presence of a nanostructured catalyst. In this particular case, product (4-AP) exhibits more chemical affinity to the Ag nanostructure than any other starting reactants. Therefore, a semi-quantitative analysis of products is performed by SERS with minimal interference from reactants. The resulting SERS signal reflects only the Raman fingerprint of product, as an amine substitute is apt to chemically absorb on Ag dendrite. Conversion of 4-NP to 4-AP is facilitated by dendrites on GaN, giving rise to gradually increased Raman signals. Raman intensity finally remain unaltered in 5 min, suggesting the fully consuming of reactant and near 100% molecular conversion rate. The kinetic study, despite of more equivocal quantification in comparison with uv-vis absorbance spectra, shows a clear trend of accumulated products on SERS-active "hotspots". Figure S2† illustrates the dependence trace of Raman intensity of signature peak at 739 cm^{-1}, 1600 cm^{-1} and 2400 cm^{-1} upon the course of reaction, subject to subtraction of background. The parallel experiment using the uv-extinction spectroscopy is performed on the identical dendrite-coated GaN substrate. As described in Figure S3†, the extinction peak near 400 nm that represents the absorption of 4-NP gradually decreased to background level, in accordance with SERS measurements in a temporal fashion. Therefore, the "one-pot" dendrite fabrication on GaN surfaces provides an excellent candidate for integration of nanostructured catalyst and *in situ* SERS detection, particularly for these

reactions under a harsh environments. Meanwhile, the simplest route for chemical synthesis renders a great potential for a large-scale manufacture, well-balancing the technical and economic needs.

REFERENCE

1. C. F. Lai, J. Y. Chi, H. C. Kuo, H. H. Yen, C. E. Lee, C. H. Chao, H. T. Hsueh and W. Y. Yeh, *Optics express*, 2009, **17**, 8795-8804.
2. C. T. Yu, W. C. Lai, C. H. Yen, H. C. Hsu and S. J. Chang, *Optics express*, 2014, **22 Suppl 3**, A633-641.
3. R. Yu, L. Dong, C. Pan, S. Niu, H. Liu, W. Liu, S. Chua, D. Chi and Z. L. Wang, *Adv Mater*, 2012, **24**, 3532-3537.
4. B. H. Chu, B. S. Kang, S. C. Hung, K. H. Chen, F. Ren, A. Sciullo, B. P. Gila and S. J. Pearton, *Journal of diabetes science and technology*, 2010, **4**, 171-179.
5. L. Sang, M. Liao, Q. Liang, M. Takeguchi, B. Dierre, B. Shen, T. Sekiguchi, Y. Koide and M. Sumiya, *Adv Mater*, 2014, **26**, 1414-1420.
6. B. Nie, B. K. Duan and P. W. Bohn, *ACS applied materials & interfaces*, 2013, **5**, 6208-6215.
7. S. Huang, Y. Zhang, B. Leung, G. Yuan, G. Wang, H. Jiang, Y. Fan, Q. Sun, J. Wang, K. Xu and J. Han, *ACS applied materials & interfaces*, 2013, **5**, 11074-11079.

8. T. L. Williamson, X. Guo, A. Zukoski, A. Sood, D. J. Diaz and P. W. Bohn, *The journal of physical chemistry. B*, 2005, **109**, 20186-20191.

9. D. Wang, A. Pierre, M. G. Kibria, K. Cui, X. Han, K. H. Bevan, H. Guo, S. Paradis, A. R. Hakima and Z. Mi, *Nano letters*, 2011, **11**, 2353-2357.

10. D. X. Wang, I. T. Ferguson and J. A. Buck, *Appl Opt*, 2009, **48**, 1178-1183.

11. H. Kim, P. E. Colavita, K. M. Metz, B. M. Nichols, B. Sun, J. Uhlrich, X. Wang, T. F. Kuech and R. J. Hamers, *Langmuir : the ACS journal of surfaces and colloids*, 2006, **22**, 8121-8126.

12. C. W. Huang, H. Y. Tseng, C. Y. Chen, C. H. Liao, C. Hsieh, K. Y. Chen, H. Y. Lin, H. S. Chen, Y. L. Jung, Y. W. Kiang and C. C. Yang, *Nanotechnology*, 2011, **22**, 475201.

13. K. B. A. Raj, K. D.; Raj, C. R. , *Chem. Mater.*, 2010, **22**, 4505.

14. M. L. M. Marin, K. L.; Scaiano, J. C., *Journal of the American Chemical Society*, 2008, **130**, 16572.

15. B. K. Duan and P. W. Bohn, *The Analyst*, 2010, **135**, 902-907.

16. K. Okamoto, I. Niki, A. Shvartser, Y. Narukawa, T. Mukai and A. Scherer, *Nature materials*, 2004, **3**, 601-605.

17. D. M. Yeh, C. F. Huang, C. Y. Chen, Y. C. Lu and C. C. Yang, *Nanotechnology*, 2008, **19**, 345201.

18. C. Y. Cho, M. K. Kwon, S. J. Lee, S. H. Han, J. W. Kang, S. E. Kang, D. Y. Lee and S. J. Park, *Nanotechnology*, 2010, **21**, 205201.

19. J. Henson, E. Dimakis, J. DiMaria, R. Li, S. Minissale, L. Dal Negro, T. D. Moustakas and R. Paiella, *Optics express*, 2010, **18**, 21322-21329.

20. K. B. R. Raj, C. R., *J of Photochem. Photobiol A: Chemistry*, 2013, **270**, 1.

21. B. K. Jena and C. R. Raj, *Langmuir : the ACS journal of surfaces and colloids*, 2007, **23**, 4064-4070.

22. Y. X. Ren, C.; Wu, M.; Niu, M.; Fang, Y., *Colloids Surf., A*, 2011, **380**, 222-228.

23. S. Kumari and R. P. Singh, *Int J Biol Macromol*, 2012, **50**, 878-883.

24. J. Xie, Q. Zhang, J. Y. Lee and D. I. Wang, *ACS nano*, 2008, **2**, 2473-2480.

25. H. Gerischer, *Electrochim Acta*, 1995, **40**, 1677-1699.

26. T. A. S. Witten, L. M., *Phys. Rev. Lett.*, 1981, **47**, 1400-1403.

27. Y. Gofer, H. Sarker, J. G. Killian, J. Giaccai, T. O. Poehler and P. C. Searson, *Biomed Instrum Technol*, 1998, **32**, 33-38.

28. S. S. Yi, L.; Lenaghan, S. C.; Wang, Y.; Chong, X.; Zhang, Z.; Zhang, M. , *RSC Advances*, 2013, **3**, 10139-10144.

29. B. Nie, R. N. Masyuko and P. W. Bohn, *The Analyst*, 2012, **137**, 1421-1427.

Captions

Scheme 1. Schematic representative of Ag dendrite growing process on GaN substrate under uv-irradiation.

Figure 1. SEM micrograph of on-chip synthesized Ag dendrite: A) in low magnification; B) high resolution scanning; C) gold nanoflower in full scope scanning; D) gold nanostructure in zoom-in scanning. UV irradiation source is from the low pressure mercury uv-lamp.

Figure 2. SEM images of silver nanostructures with different irradiation time. A) polyhedral cube in low magnification, 1 min; B) singlet polyhedral nanocube with high resolution scanning, 3 min; C) short dendroid structure from rectangle edge, 5 min; D) hyper-branched dendrite on planar GaN, 8min.

Figure 3. Enhanced Raman spectra of different analysts: (A) Rhodamine 6G and virgin GaN (blue dot); (B) 4-aminothiophenol. Laser excitation wavelength of 532.8nm.

Figure 4. A series of SERS spectra obtained after different reaction time over the progress of catalytic reduction of 4-NP, a) 0s, b)100s, c)200s, d)300s, respectively, exhibiting the gradual increase of Raman intensity. The spectra are subject to offset for decent clarity.

Reagent-free Photochemical Silver Dendrite Synthesis on Gallium Nitride Thin Film as a SERS-active Substrate and Catalytic Cluster

Bei Nie[a,b*], Qiuhong Zhou[a] and Weiling Fu[b]

[a.] Chongqing Institute of Green and Intelligent Technology, Chinese Academy of Science, P. R. China

[b.] Department of Clinical Diagnostics and Therapeutics, Xinan Hospital, Third Military Medical University, Chongqing, P. R. China

Captions

Scheme 1. Schematic representative of Ag dendrite growing process on GaN substrate under uv-irradiation.

Figure 1. SEM micrograph of on-chip synthesized Ag dendrite: A) in low magnification; B) high resolution scanning; C) gold nanoflower in full scope scanning; D) gold nanostructure in zoom-in scanning. UV irradiation source is from the low pressure mercury uv-lamp.

Figure 2. SEM images of silver nanostructures with different irradiation time. A) polyhedral cube in low magnification, 1 min; B) singlet polyhedral nanocube with high resolution scanning, 3 min; C) short dendroid structure from rectangle edge, 5 min; D) hyper-branched dendrite on planar GaN, 8min.

Figure 3. Enhanced Raman spectra of different analysts: (A) Rhodamine 6G and virgin GaN (blue dot); (B) 4-aminothiophenol. Laser excitation wavelength of 532.8nm.

Figure 4. A series of SERS spectra obtained after different reaction time over the progress of catalytic reduction of 4-NP, a) 0s, b)100s, c)200s, d)300s, respectively, exhibiting the gradual increase of Raman intensity. The spectra are subject to offset for decent clarity.

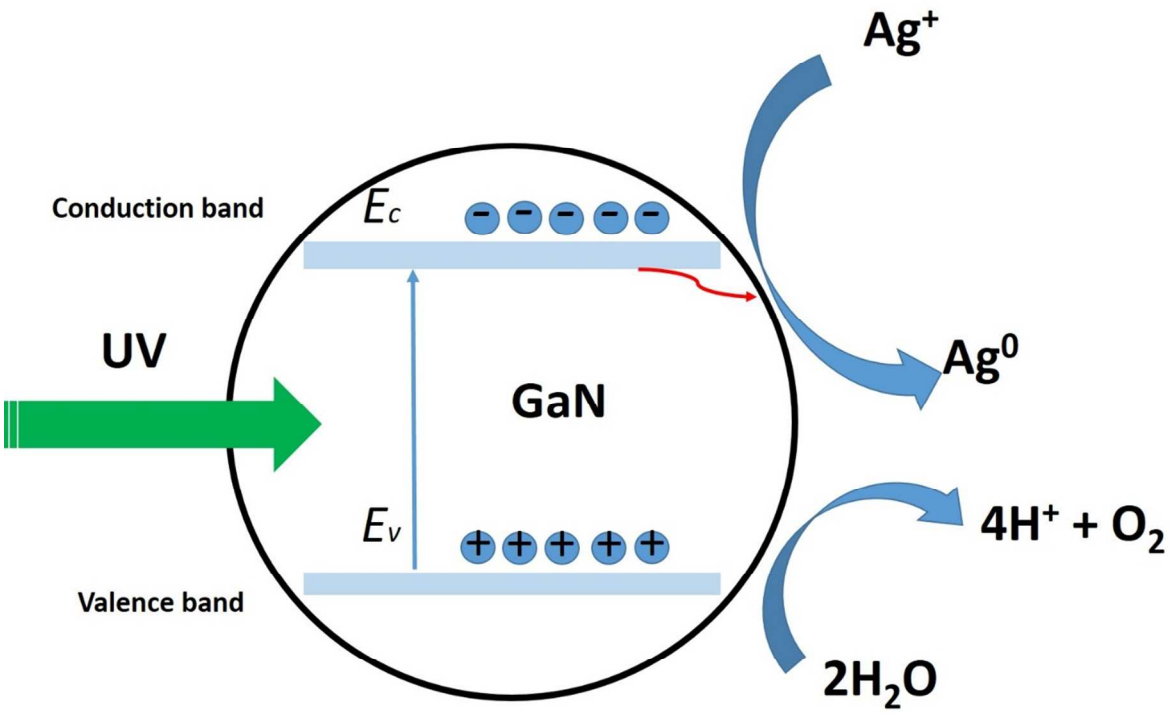

Scheme 1. Schematic representative of Ag dendrite growing process on GaN substrate under uv-illumination.

Figures

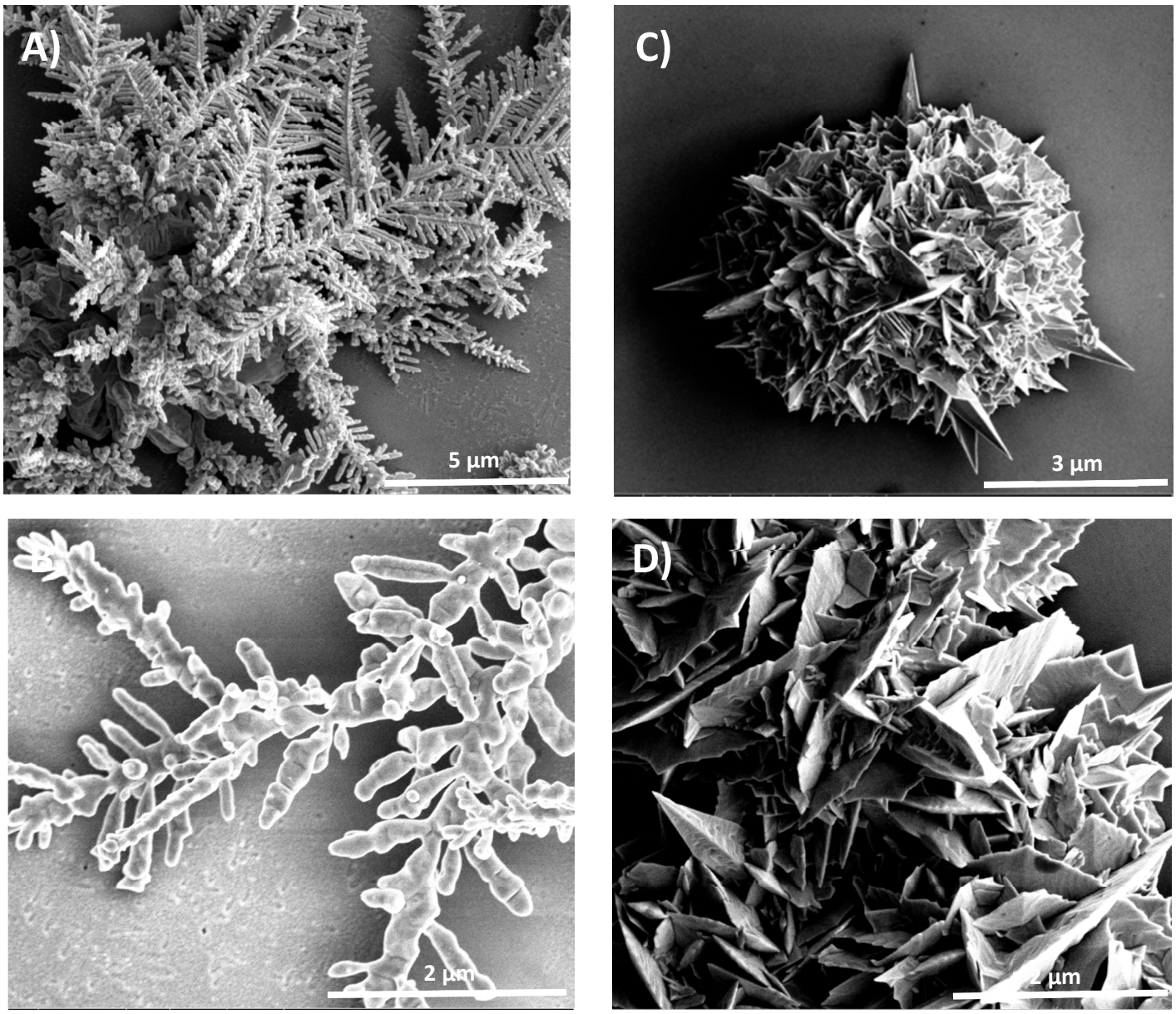

Figure 1. SEM micrograph of on-chip synthesized Ag dendrite: A) in low magnification; B) high resolution scanning; C) gold nanoflower in full scope scanning; D) gold nanostructure in zoom-in scanning. UV irradiation source is from the low-pressure mercury uv-lamp.

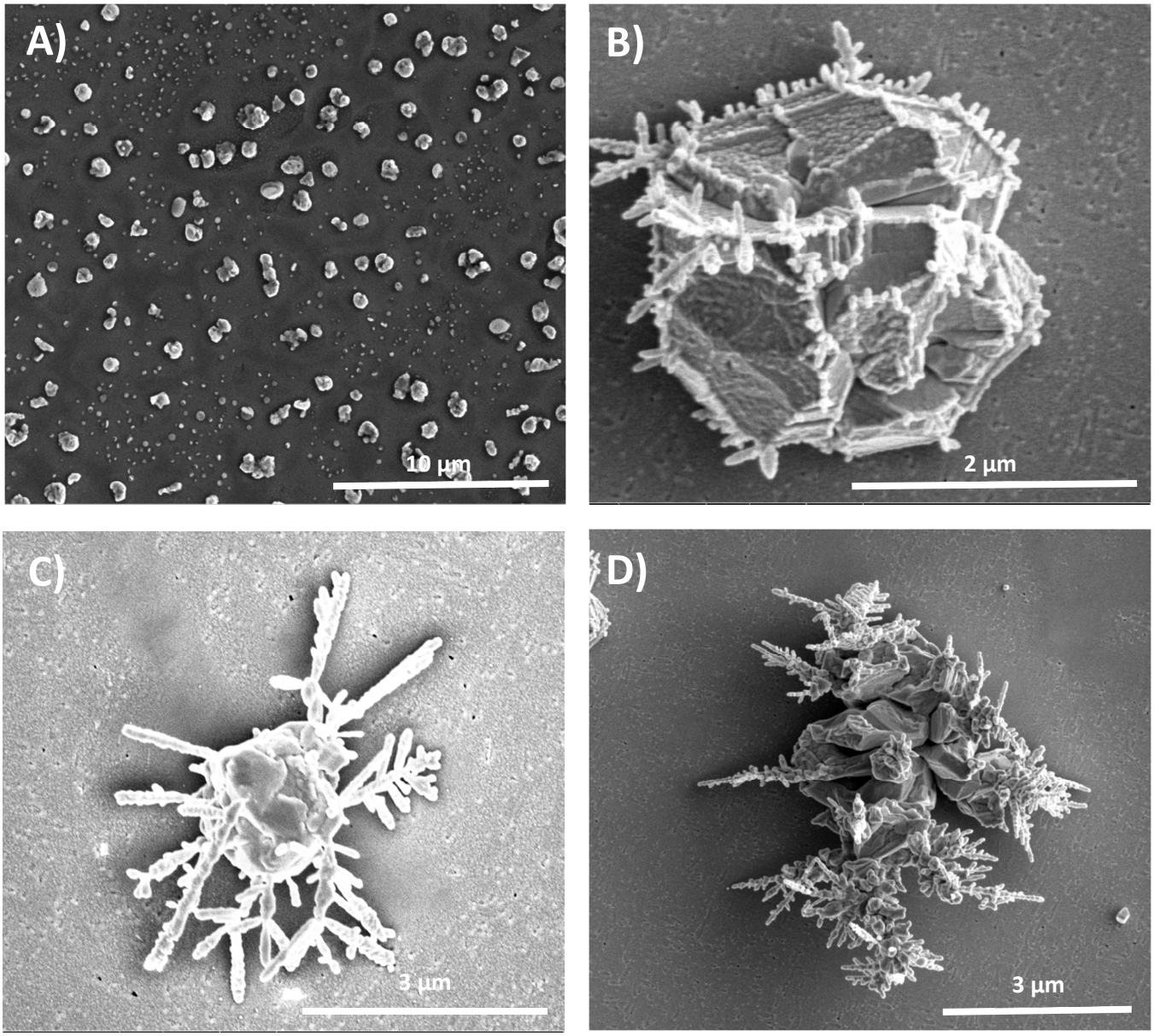

Figure 2. SEM images of silver nanostructures with different irradiation time. A) polyhedral cube in low magnification, 1 min; B) singlet polyhedral nanocube with high resolution scanning, 3 min; C) short dendroid structure from rectangle edge , 5 min; D) hyper-branched dendrite on planar GaN, 8 min.

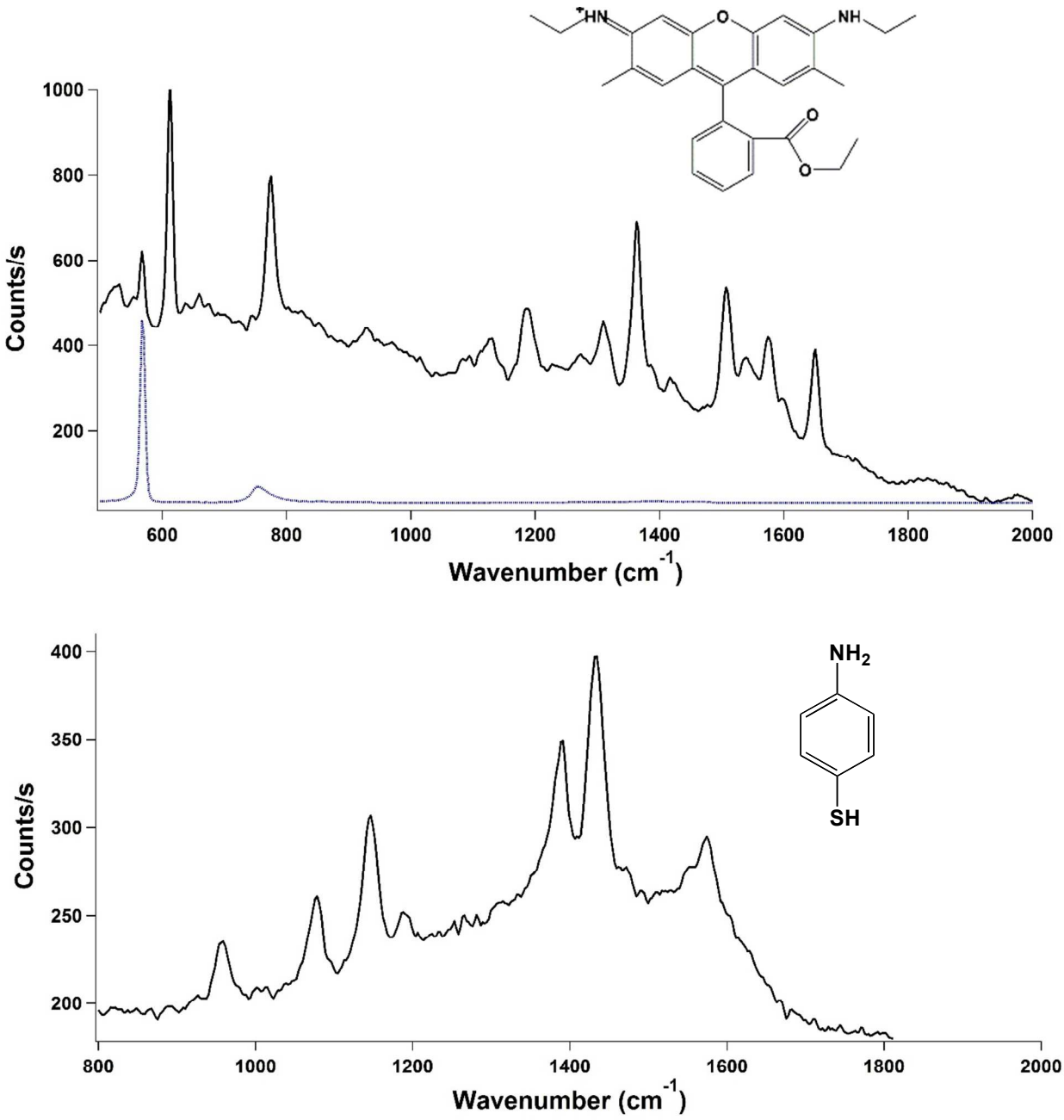

Figure 3. Enhanced Raman spectra of different analysts: (A) Rhodamine 6G and virgin GaN (blue dot), (B) 4-aminothiophenol. Laser excitation wavelength of 532.8 nm.

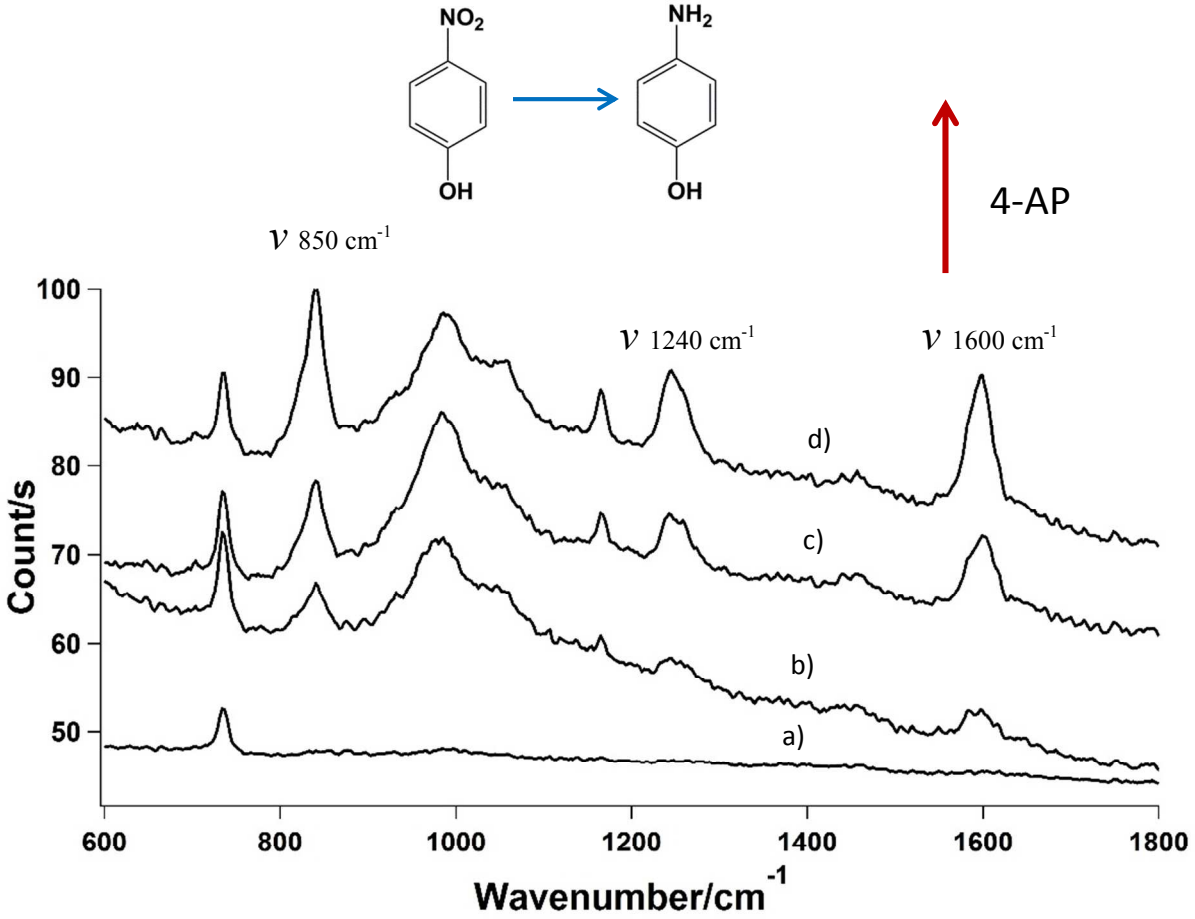

Figure 4. A series of SERS spectra obtained after different reaction time over the progress of catalytic reduction of 4-NP, a) 0s, b)100s, c)200s, d)300s, respectively, exhibiting the gradual increase of Raman intensity. The spectra are subject to offset for decent clarity.